JOURNAL OF SOLID STATE CHEMISTRY 60, 214–229 (1985)

Anhydrous Deuterium β-Alumina: Powder Neutron Diffraction Studies at 4.2, 298, 573, and 720 K

JOHN M. NEWSAM* AND ANTHONY K. CHEETHAM

Chemical Crystallography Laboratory, Hooke Building, 9 Parks Road, Oxford, OX1 3PD, United Kingdom

AND BRUCE C. TOFIELD

Materials Development Division, Building 552, AERE Harwell, Oxon, OX11 ORA, United Kingdom

Received February 11, 1985; in revised form May 6, 1985

The structure of anhydrous stoichiometric deuterium β-alumina, $DAl_{11}O_{17}$, has been determined at 4.2, 298, 573, and 720 K by profile refinement of powder neutron diffraction data. At each temperature the deuterium is found to lie in well-defined threefold sites close to the spacer oxygen, O(5). There is no evidence for delocalization of the deuterium away from O(5) and such a hydroxyl linkage is in accord with the low protonic conductivity observed in related materials. The effect of this unusual mirror-plane arrangement on the remainder of the structure and the variation with temperature of the lattice constants, bond lengths, and angles are discussed.

1. Introduction

Interest in compounds of the β-alumina family stems primarily from their remarkable ionic conducting properties (*1*). These materials have the general formula $M_{1+x}Al_{11}O_{17+x/2}$ and adopt space group symmetry $P6_3/mmc$. For sodium β-alumina, $a = 5.60$ Å and $c = 22.53$ Å (*2*). The length of the c axis depends both on the level of nonstoichiometry, x,[1] and on the nature of the counterion, M (*9*) (for recent reviews see Refs. *3* and *4*).

A consequence of the mobility of sodium and other ions in β-alumina is that derivatives can readily be prepared by ion exchange in an appropriate molten salt. Protons may be introduced quantitatively into the mirror planes by three methods (*3, 10–12*). These involve the exchange of Na^+ by NH_4^+ or "H_3O^+" in molten ammonium nitrate or hot concentrated sulfuric acid, respectively, and the direct reduction of silver β-alumina by hydrogen at ca. 450°C. Hydrogen-containing materials are chemically of great interest in that they offer a preparative route to more nearly stoichiometric materials, $MAl_{11}O_{17}$ (*7, 8, 13*).

The β-alumina structure consists of closely-packed slabs, termed spinel blocks, which are separated by planes of crystallographic mirror symmetry. These mirror planes contain the spacer oxygen O(5) and

* Present address: Exxon Research and Engineering Company, Clinton Township, Route 22 East, Annandale, New Jersey 08801.

[1] For both sodium (*1, 5*) and silver (*6–8*) β-aluminas the c axis lattice constant decreases with increasing x.

0022-4596/85 $3.00

the monovalent cations (Fig. 1). The basic framework is thus relatively refractory, and hydrogen-containing β-aluminas were therefore considered as potential proton conductors at elevated temperatures, a view supported by some earlier work (*14, 15*). Normally (*16*), proton conductors such as $HClO_4 \cdot H_2O$ (*17*) and $HUO_2PO_4 \cdot 4H_2O$ (*18*) have only limited thermal stability.

Kummer (*9*) first investigated the reduction of $Ag_{1+x}Al_{11}O_{17+x/2}$ by hydrogen and found that, after partial reaction, a band at 3520 cm^{-1} appeared in the infrared spectrum. A more recent infrared study (*19*) revealed a similar frequency of 3510 cm^{-1} for this vibration which, in the light of structural results, was assigned (*19*) to an in-plane O(5)–H stretching mode.

Tofield *et al.* (*20*) examined a polycrystalline sample of deuterium β-alumina at 4.2 K and 550°C using powder neutron diffraction. At 4.2 K, the deuterium was found to be bonded to the spacer oxygen at a distance of 0.98 Å. This novel arrangement for a β-alumina was seen as responsible for the increased length of the *c* axis, 22.619 Å, as well as influencing the bond lengths about Al(3) adjacent to the mirror plane. Further, the occupation number for deuterium, 0.87(5), was close to that of the stoichiometric composition, $x = 0$, although the sodium β-alumina synthesized as the precursor was highly nonstoichiometric with $x = 0.45$. At 550°C, the deuterium could not be located within the mirror planes, giving rise to optimism about the possible proton conductivity (*14*). Somewhat surprisingly, at 550°C the *c* axis had contracted to 22.611 Å. At the time, the possibility of a reverse exchange to silver β-alumina was rejected, because of the much longer *c* axis compared to nonstoichiometric silver β-alumina (22.49 Å at room temperature (*6*)) and the absence of significant scattering density around the *aBR* site which is occupied by silver in the nonstoichiometric material. We have recently demonstrated, however, that reverse exchange had indeed occurred (*21*) at the higher temperature. The stoichiometric silver β-alumina prod-

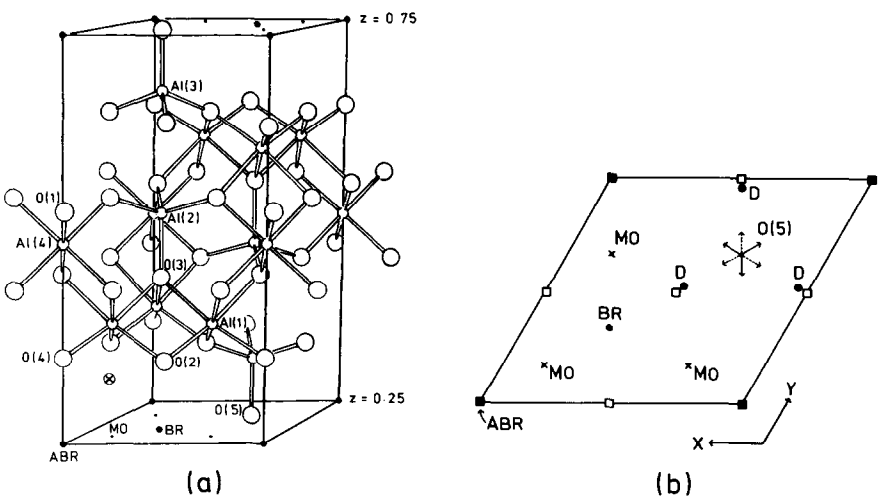

FIG. 1. A schematic diagram of the β-alumina structure. The conventional atom numbering scheme is shown at left (a), together with the nomenclature for sites within the crystallographic mirror planes at $z = \frac{1}{4}$ and $z = \frac{3}{4}$. The right portion, (b), is a representation of the $z = \frac{1}{4}$ mirror plane in the structure of $DAl_{11}O_{17}$. The projections of the bordering O(2) (□) and O(4) (■) atoms and the two possible displacements of O(5) to 6*h* sites (solid and dashed lines) are indicated.

uct has since been studied as a function of temperature (*8, 22*).

The present study was undertaken to resolve some of the ambiguities about the stoichiometry and structure of deuterium β-alumina and to study the evolution of the structure with temperature in detail. We chose a more typical starting composition of $x = 0.3$ and we have determined the structure of the resulting deuterium beta alumina at 4.2, 298, 573, and 720 K using powder neutron diffraction data.

2. Experimental

The samples were prepared in the same manner as described previously (*20*). Monofrax sodium β-alumina, of approximate composition $Na_{1.3}Al_{11}O_{17.15}$, was ground by hand in an agate mortar to a fine powder, meshed at 37 μm, and converted to silver β-alumina by two exchanges in a large excess of molten silver nitrate at ~300°C. The nonstoichiometric silver β-alumina product was washed and dried under vacuum at ~350°C. Reduction was effected by deuteration (D_2: Air Products, >99.9%) at 450°C in a sealed silica system.[2] Under these conditions, as described previously (*20, 21*), the deuterium is rapidly absorbed with the liberation of silver metal which forms a coating on the surface of the crystallites. During the preparation moisture is evolved, apparently reflecting conversion to the stoichiometric material according to

$$Ag_{1.3}Al_{11}O_{17.15} + 0.65D_2 \rightarrow DAl_{11}O_{17} + 0.15D_2O + 1.3Ag. \quad (1)$$

The moisture was pumped off and more deuterium admitted several times until no further pressure change was observed.

[2] Deuterium is chosen in place of hydrogen to facilitate the subsequent neutron scattering measurements—hydrogen has a smaller coherent scattering length and a large incoherent scattering contribution.

The sealed reaction vessel was then moved to a dry glove box and the product transferred to a 15-mm diameter vanadium can which was tightly sealed with a gold O-ring. In the earlier experiments (*20*), the degree of seal integrity required to prevent D_2 loss and consequent reintroduction of silver into the structure on heating had not been appreciated. In air, this reverse exchange is found to occur at ~300°C. In the experiments described here, a gas-tight seal was maintained.

It is possible to remove the surface coating of silver metal (Reaction (1)) by treatment with nitric acid (*23*). Such treatment, however, allows the introduction of water and/or exchange by hydrated species. The silver metal does not pose a serious problem in neutron diffraction studies and therefore, following the preparation, the silver-containing sample was maintained under anhydrous conditions.

Powder neutron diffraction measurements were performed on the PANDA diffractometer at AERE Harwell. A mean neutron wavelength of 1.5172 Å was selected from the [511] planes of a Ge monochromator at a take-off angle of 88°. This wavelength was accurately calibrated by a peak-fitting of the 111, 200, 220, and 311 reflections from a standard nickel powder sample.

For the scan at 4.2 K, the sample can was immersed in liquid helium using a TBT Associates cryostat. At room temperature, the sample was mounted on goniometer arcs, and for temperatures above ambient, an evacuable furnace with a tantalum heating element was used. In each case, the height of the sample can was adjusted with reference to the direct beam.

On PANDA, three counters in the diffracting plane at approximately 5° separation in 2θ are available for data collection. The region of 2θ available to the low-angle counter, from 6 to 104.5° was scanned in increments of 0.1°. The measurement time

determined by a fission counter monitor was ~220 sec (4.2, 573, and 720 K) or ~140 sec (298 K) for each point. The situation of the PANDA diffractometer was at the time such that the counters were susceptible to occasional bursts of extraneous radiation. To enable the resulting spurious points in the PND pattern to be recognized and corrected, the data from each of the three equatorial counters were plotted individually. For each run, the data from these three counters were then collated to yield the complete profile in the range $6 \leq 2\theta \leq 114.5°$.

The data were analyzed by full-matrix least-squares fitting of the calculated diffraction profile to the observed profile using the computer program originally written by Rietveld (*24*) and modified by Clarke (*25, 26*). Scattering lengths of 0.345, 0.583, 0.60, and 0.667 (all $\times 10^{-14}$ m) were used for Al (*27*), O (*27*), Ag (*28*), and D (*28*), respectively. Space group symmetry $P6_3/mmc$ (No. 194) was assumed and confirmed by the subsequent analysis. During refinement, the region $2\theta \leq 25°$ or 30° was omitted from the calculations because the peak shapes at low Bragg angles show marked deviations from ideal Gaussian. The areas within which reflections from the silver metal impurity contributed appreciable intensity were also excluded (~5° 2θ in all). For the runs at 573 and 720 K, three peaks were observed from the Ta element of the furnace, necessitating the exclusion of a further 1.5° 2θ (see Fig. 7).

3. Results

3.1. 4.2 K

In the previous study, the deuterium location was revealed (*20*) by an $|F_{obs}|$ Fourier synthesis based on a phasing model of the atomic coordinates of the spinel block atoms and of the spacer oxygen, O(5). With the present data set, these coordinates were then optimized in the initial refinements together with the scale, cell, and instrumental parameters. In the corresponding Fourier syntheses, however, the only additional features that were apparent were found to be spurious in subsequent refinement. Further, in all of the powder experiments described here observed or difference Fourier techniques were not helpful in initial structure elucidation. The definition in the picture of scattering density provided by a Fourier synthesis is determined by the number and accuracy of scattering amplitudes and their phases. Compared with a single-crystal diffraction experiment, data from powder samples suffer from intrinsically lower signal-to-noise, from our inability to extract unique intensities from coincident or overlapped peaks, and from the method generally used to deconvolute the pattern which biases the observed phases and intensities strongly toward the calculated model. These constraints, together with series-termination errors, combine to limit the applicability of Fourier techniques in analyzing powder diffraction data. However, although the experiences described here are relatively typical, there are examples where observed or difference Fourier syntheses have been used successfully in structure determination (*20, 29*). We anticipate that the potential use of these techniques will benefit greatly from the improved resolution that will be provided by the next generation of synchrotron X-ray and neutron powder diffractometers.

Following the lack of success of the Fourier trials, a deuterium atom was introduced at the position reported previously (*20*), and iterative least-squares procedures were used to improve all the atomic and instrumental parameters. A correction for preferred orientation was considered in several refinements, but the parameter (*24*) converged to a low value for both this and the other data sets collected at higher tem-

peratures and the correction was, therefore, subsequently discarded. The structural parameters which emerged were in good agreement with those reported by Tofield *et al.* (*20*). There was no evidence for occupation of any mirror-plane sites other than those of deuterium close to O(5) and of the spacer oxygen itself. For example, the occupation number of a silver atom entered at the stoichiometric silver position (*8*), $x\ 2x\ \frac{1}{4}$ (*6h*); $x = 0.776$, converged to 0.07(7). Further, although our starting composition was slightly less soda-rich, a deuterium occupation close to unity was found.

The final details of the spacer oxygen and deuterium sites do, however, differ. In the previous refinement, an unequivocal distinction between 6*h* and 12*j* ($x\ y\ \frac{1}{4}$) sites for D and O(5) could not be made, and the 12*j* site was tentatively chosen as the preferred location by reference to the Fourier map (Fig. 3 of Ref. (*20*)) and the apparent bond distances in the different models. The present work reveals the 6*h* type site to be that actually occupied by both deuterium and the spacer oxygen. Combinations of two types of deuterium site (6*h*: $x\ \bar{x}\ \frac{1}{4}$ and 12*j*: $x\ y\ \frac{1}{4}$) and three types of O(5) sites (6*h*: $x\ \bar{x}\ \frac{1}{4}$, $x < \frac{1}{3}$, 6*h*: $x\ \bar{x}\ \frac{1}{4}$, $x > \frac{1}{3}$ and 12*j*: $x\ y\ \frac{1}{4}$) were tested in least-squares refinements. Displacement of either/both O(5) or/and D away from the threefold 6*h* sites to the 12*j* positions which are separated by the $x\ \bar{x}\ z$ mirror plane gave less satisfactory agreements than models involving only the 6*h* sites. Further, many of these refinements were unstable and in some the D–O(5) bond length was unreasonably long.

A distinction between the two senses of displacement of O(5) away from the 2*c* special position was less clear (Fig. 1). The residuals for the refinement which converged at $x_O = 0.2965$ were essentially identical to those for $x_O = 0.3712$. (Note that the extent of the displacement from the 2*c* site is the same in both cases). However, the corresponding O–H bond lengths were 1.19 and 1.06 Å, respectively. The infrared O(5)–H stretching frequency of 3510 cm^{-1} (*19*) points toward a bond length of ~1 Å (*30*), and there is thus little doubt that the latter 6*h* site with $x_O > \frac{1}{3}$ most correctly models the actual structure. This displacement of O(5) is in the same sense as found previously (*20*) and is unusual in that the displacement is generally toward the *aBR* site rather than toward the BR site. The latter displacement, observed here, may be explained in terms of a weak interaction O(5)–H . . . O(2), and a similar effect has been observed in an X-ray structure refinement (*31, 32*) of hydrogen-containing β-alumina. In that case (*3*) the hydrogen bonding scheme O(5)–H . . . OH_2 is slightly different in that the second oxygen at the Beevers–Ross position is that of a water molecule.

We were also able to introduce anisotropic temperature factors for all atoms at each of the four temperatures studied (*33*). Generally, no relaxation factors were necessary and instabilities occurred only when some particular displacements of deuterium and O(5) away from the 6*h* special positions were considered. However, in each case the vibrations of the spinel block atoms are well described by isotropic components and, with the limited amount of data, significant improvements in the residuals were not obtained by using fully anisotropic components (*33*). In the final stages of refinement, therefore, such components were retained only for the mirror plane constituents as these might be expected to show pronouncedly anisotropic behavior.

The final residuals and instrumental and overall parameters are listed in Table I, with final atomic parameters in Table II. The corresponding bond lengths and angles are presented in Tables III and IV.

Figure 2 displays the $z = 0.25$ sections of $|F_{obs}|$ and $|F_{obs} - F_{calc}|$ Fourier syntheses computed using structure factors derived from these final refinements of the 4.2 K

TABLE I

FINAL OVERALL PARAMETERS WITH ESTIMATED STANDARD DEVIATIONS IN PARENTHESES

	Temperature (K)			
	4.2	298	573	720
R_f[a]	0.0753	0.0797	0.0710	0.0784
R_p	0.1373	0.1219	0.1385	0.1361
R_{WP}	0.1051	0.0963	0.1009	0.1014
R_E	0.0932	0.0977	0.0943	0.0990
N_{ref}[b]	174	176	165	182
a A	5.6008(6)	5.6037(5)	5.6137(6)	5.6173(6)
c A	22.6118(10)	22.6169(8)	22.6424(9)	22.6483(9)
V A^3	614.3(2)	615.1(2)	618.0(2)	618.9(2)
$z\theta$[c]	18.4(3)	17.5(2)	17.4(3)	16.0(3)
U	3570(211)	2327(154)	2590(197)	2571(192)
V	−4323(275)	−2741(205)	−3088(253)	−3039(246)
W	2065(88)	1573(67)	1687(80)	1681(77)

[a] The definitions of the various residuals are as given in Ref. (*24*).

[b] N_{ref} is the number of reflections which contribute to the observed profile used in refinement (see Figs. 3, 4, 8, and 9).

[c] The counter zero-point error, $z\theta$, and the halfwidth parameters, U, V, and W are expressed in units of one hundredth of a degree in 2θ.

data. In contrast to the $/F_{obs}/$ syntheses mentioned above, substantial scattering density corresponding to deuterium is now apparent. However, as in the previous analysis (*20*), the atomic distribution appears quite diffuse about the $x\ \bar{x}\ z$ mirror plane. As we see below, the misleading appearance derives from the approximate nature of the $/F_{obs}/$ Fourier calculations. No significant features were apparent in any of the difference Fourier sections although the errors inherent in the derived structure factors are such that it is unlikely that, say, slight occupation of the interstitial aluminum site would be apparent in such a synthesis. The final observed and calculated diffraction profiles are shown in Fig. 3.

3.2. 298 K

The course of structure analysis paralleled that for the 4.2 K data. Similar structural models were optimized by full-matrix least squares as outlined above, with anisotropic temperature factors being introduced for O(5) and D in later stages. Displacements of O(5) and D to 12*j* positions were also considered. Such a shift for O(5) always gave slightly worse agreements and, for D, a similar situation occurred, with, in each case, the deuterium coordinates converging close to the 6*h* position. A displacement away from the mirror plane to a 12*k* position, $x\ \bar{x}\ z$, also gave poorer fits. The 6*h* sites were therefore again taken to represent most accurately the actual situation within the structure.

The final observed and calculated diffraction profiles are displayed in Fig. 4. The final residuals of $R_P = 0.1219$, $R_{WP} = 0.0963$ are slightly better than those obtained with the other data sets (Table I) despite the shorter time spent in data collection. This probably reflects the improvement in data quality which results when the incident and diffracted beams do not have to pass

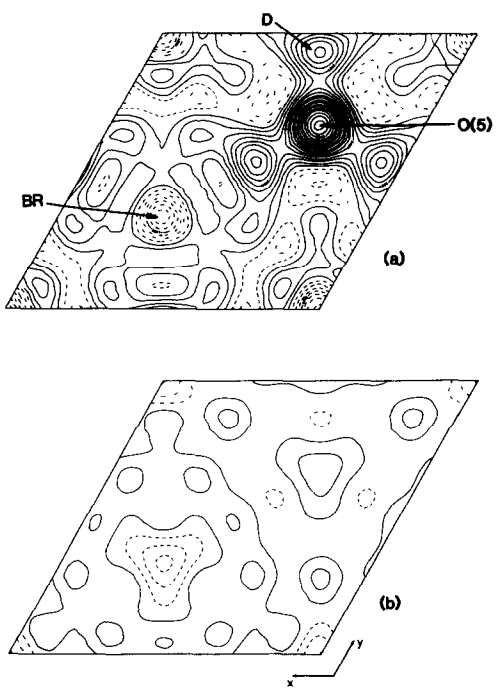

FIG. 2. The $z = \frac{1}{4}$ sections of $/F_{obs}/$ ((a) upper) and $/F_{obs} - F_{calc}/$ ((b) lower) Fourier syntheses using structure factors derived from the final profile refinements of $DAl_{11}O_{17}$ at 4.2 K. Both sections are on the same absolute scale and have the same contour levels. The contours are marked in arbitrary units.

TABLE II

FINAL ATOMIC PARAMETERS WITH ESTIMATED STANDARD DEVIATIONS IN PARENTHESES

	Temperature (K)	x	y	z	Occn.[a]	B or U_{11}[b]	U_{33}	U_{12}
O(1)	4.2	0.1577(8)	$2x$	0.0492(2)	6.0	0.3(1)		
12*k*[c]	298	0.1575(6)		0.0494(2)		0.2(1)		
m[d]	573	0.1597(10)		0.0495(2)		1.1(1)		
	720	0.1590(9)		0.0495(2)		1.2(1)		
O(2)	4.2	0.5011(9)	$2x$	0.1450(2)	6.0	0.3(1)		
12*k*	298	0.5007(7)		0.1457(1)		0.3(1)		
m	573	0.5012(9)		0.1455(2)		0.7(1)		
	720	0.4987(8)		0.1456(2)		0.7(1)		
O(3)	4.2	$\frac{2}{3}$	$\frac{1}{3}$	0.0572(4)	2.0	0.2(2)		
4*f*	298			0.0564(4)		0.3(2)		
3*m*	573			0.0556(5)		0.4(2)		
	720			0.0563(4)		0.3(2)		
O(4)	4.2	0	0	0.1421(6)	2.0	0.6(2)		
4*e*	298			0.1396(4)		0.7(2)		
3*m*	573			0.1403(6)		1.2(3)		
	720			0.1410(6)		1.8(2)		
O(5)	4.2	0.372(2)	$\bar{x}$	$\frac{1}{4}$	1.0	−0.011(17)[e]	0.034(15)	0.014(9)
6*h*	298	0.370(5)				0.031(29)[e]	0.036(13)	0.036(17)
mm	573	0.298(12)				0.049(57)	0.055(21)	0.033(26)
	720	0.296(5)				0.040(34)	0.057(18)	0.036(20)
Al(1)	4.2	0.8336(16)	$2x$	0.1067(3)	6.0	0.5(1)		
12*k*	298	0.8357(12)		0.1065(2)		0.4(1)		
m	573	0.8325(17)		0.1068(3)		0.6(1)		
	720	0.8326(15)		0.1073(3)		0.7(1)		
Al(2)	4.2	$\frac{1}{3}$	$\frac{2}{3}$	0.0238(6)	2.0	0.1(2)		
4*f*	298			0.0237(5)		0.3(2)		
3*m*	573			0.0249(6)		0.2(2)		
	720			0.0243(5)		−0.4(2)[e]		
Al(3)	4.2	$\frac{1}{3}$	$\frac{2}{3}$	0.1694(7)	2.0	0.2(3)		
4*f*	298			0.1708(6)		1.0(2)		
3*m*	573			0.1690(7)		0.6(3)		
	720			0.1679(7)		1.2(3)		
Al(4)	4.2	0	0	0	1.0	−0.6(3)[e]		
2*a*	298					−0.4(3)[e]		
$\bar{3}m$	573					0.3(3)		
	720					1.1(4)		
D	4.2	0.467(4)	$\bar{x}$	$\frac{1}{4}$	1.2(1)	0.092(23)	0.018(13)	0.077(19)
6*h*	298	0.464(3)			1.0(1)	0.056(17)[e]	0.042(16)	0.060(14)
mm	573	0.458(4)			0.9(2)	0.099(37)[e]	0.078(31)	0.103(33)
	720	0.454(3)			1.2(2)	0.142(36)	0.151(36)	0.145(31)

[a] Occupation numbers are expressed as comprising the $DAl_{11}O_{17}$ unit which is half the content of one unit cell.

[b] Anisotropic temperature factors for O(5) and D are given in the form: $\exp[-2\pi^2(U_{11}(h^2 + k^2)a^{*2} + U_{33}l^2c^{*2} + 2U_{12}hka^*b^*)]$.

[c] Wyckoff notation.

[d] Site symmetry.

[e] These temperature factor matrices are not positive definite. This probably derives from minor errors in background estimation at higher angles, a relatively common problem in powder profile refinements. In each case a maximum correction of twice the estimated standard deviation is sufficient to make the matrix positive definite. Such corrections have been made in producing Fig. 11.

TABLE III

CALCULATED BOND LENGTHS (Å) WITH ESTIMATED STANDARD DEVIATIONS[a] IN PARENTHESES

		Temperature (K)				
	Number of bonds	4.2[b]	4.2	298	573	720
			Octahedra			
Al(1)–O(1)	2	2.037(5)	2.042(8)	2.028(5)	2.053(9)	2.059(9)
–O(2)	2	1.826(6)	1.830(7)	1.851(6)	1.834(9)	1.841(9)
–O(3)	1	1.989(7)	1.968(8)	1.995(7)	1.985(9)	1.986(9)
–O(4)	1	1.793(7)	1.801(9)	1.761(7)	1.797(10)	1.799(10)
av. Al(1)–O		1.918(2)	1.919(3)	1.919(2)	1.926(4)	1.931(4)
Al(4)–O(1)	6	1.879(5)	1.892(7)	1.894(5)	1.915(8)	1.911(7)
			Tetrahedra			
Al(2)–O(1)	3	1.826(7)	1.797(8)	1.803(7)	1.777(9)	1.790(8)
–O(3)	1	1.801(15)	1.832(15)	1.810(15)	1.825(17)	1.824(16)
av. Al(2)–O		1.820(5)	1.806(5)	1.805(5)	1.789(6)	1.799(5)
Al(3)–O(2)	3	1.751(5)	1.719(6)	1.721(5)	1.717(7)	1.687(7)
–O(5)	1	1.796(16)	1.861(6)	1.827(8)	1.866(10)	1.894(8)
av. Al(3)–O		1.762(4)	1.755(3)	1.748(3)	1.754(4)	1.739(4)
			Deuterium contacts			
D–O(5)		0.98(5)	0.92(1)	0.91(2)	1.08(3)[c]	1.04(2)[c]
–O(2)		—	2.397(8)	2.386(5)	2.403(9)	2.404(8)
–Al(3)		—	2.23(1)	2.20(1)	2.20(2)	2.20(1)

[a] The esd's presented here are manual estimates derived from the esd's of the atomic coordinates and they therefore merely provide a guide toward the reliability of each value.

[b] Data from Tofield *et al.* (Ref. (*20*)).

[c] The symmetry operator $(\bar{y}, x - y - 1, z)$ has been applied to D.

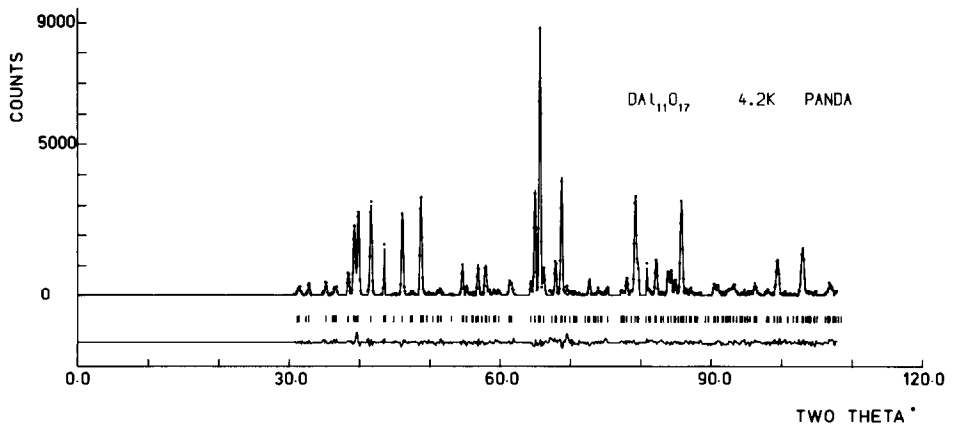

FIG. 3. The final observed (dots), calculated (continuous line), and difference (lower) diffraction profiles for $DAl_{11}O_{17}$ at 4.2 K. The positions of the contributing reflections are marked by bars.

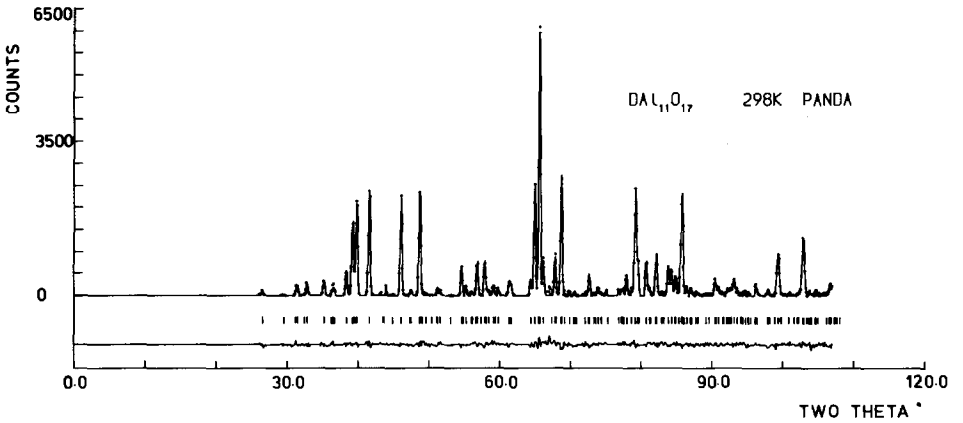

FIG. 4. The final observed, calculated, and difference diffraction profiles for $DAl_{11}O_{17}$ at 298 K (legend as for Fig. 3).

through the apparatus which is required for temperature control.

The $z = 0.25$ sections of $/F_{obs}/$ and $/F_{obs} - F_{calc}/$ Fourier syntheses are depicted in Fig. 5. The definition is striking and is a further consequence of the improved quality of the

TABLE IV

CALCULATED BOND ANGLES WITH ESTIMATED STANDARD DEVIATIONS[a] IN PARENTHESES

	Temperature (K)				
	4.2[b]	4.2	298	573	720
		Octahedra			
O(1)–Al(1)–O(1)	79.7(3)	80.9(5)	81.5(4)	81.8(7)	81.2(6)
–O(2)	90.4(2)	89.6(3)	89.9(3)	89.3(7)	88.8(5)
–O(3)	88.5(3)	88.8(5)	88.5(4)	88.2(8)	88.2(7)
–O(4)	83.5(3)	84.8(4)	84.2(3)	83.7(6)	83.9(6)
O(2)–Al(1)–O(2)	98.7(4)	98.9(5)	97.8(5)	98.9(7)	100.5(6)
–O(3)	85.1(2)	84.4(4)	84.3(3)	85.5(5)	85.5(5)
–O(4)	101.6(3)	101.0(5)	101.8(4)	101.4(7)	101.1(7)
O(3)–Al(1)–O(4)	—	171.7(6)	170.4(5)	169.4(9)	169.5(8)
O(1)–Al(4)–O(1)	88.0(2)	88.9(4)	88.7(3)	89.2(6)	89.0(5)
		Tetrahedra			
O(1)–Al(2)–O(1)	110.2(5)	110.3(6)	110.1(5)	110.7(9)	110.3(9)
–O(3)	108.7(4)	108.6(5)	108.8(5)	108.2(9)	108.6(8)
O(2)–Al(3)–O(2)	108.1(6)	110.2(7)	109.7(6)	110.8(11)	111.4(11)
–O(5)	—	97.0(9)	97.9(8)	102.5(13)[c]	101.7(13)[c]
–O(5)′	113.1(11)	114.3(9)[c]	114.6(8)[c]	118.8(12)	118.6(11)
		Deuterium contacts			
Al(3)–O(5)–D	—	101.7(12)	101.3(12)	92.6(15)[d]	92.4(15)[d]

[a] The esd's were derived as given in the note to Table III.

[b] Data of Tofield *et al.* (Ref. (*20*)).

[c,d] The symmetry operator $(\bar{y}, x - y - 1, z)$ has been applied to O(5) (*c*) or D (*d*), respectively.

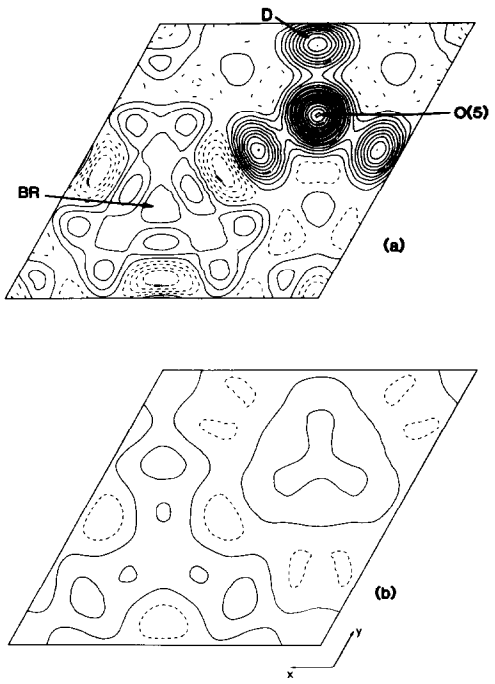

FIG. 5. The $z = \frac{1}{4}$ sections of $/F_{obs}/$ ((a) upper) and $/F_{obs} - F_{calc}/$ ((b) lower) Fourier syntheses calculated using structure factors derived from the final profile refinements of $DAl_{11}O_{17}$ at 298 K (details as for Fig. 2).

observed data set. The deuterium is clearly seen to lie on the $x\ \bar{x}$ mirror plane, the 6*h* site. As the atomic distributions at 4.2 and 298 K are essentially identical (Table II), the improved residuals for the 298 K data set suggest that Fig. 5a depicts this distribution more accurately than the corresponding section derived from the 4.2 K data set (Fig. 2a).

3.3. 573 and 720 K

Analysis of the data collected at 573 and 720 K followed the same paths as those for the earlier data sets. The silver metal reflections were still apparent in the measured diffraction profile and they were of similar relative intensities to those observed at 4.2 and 298 K. The back exchange to $AgAl_{11}O_{17}$ had, therefore, been avoided. Two differences between the high- and low-temperature data were, however, apparent.

First, the lattice constants, which displayed only a slight expansion from 4.2 to 298 K, had increased substantially (Table I). The data sets were collected consecutively, with no alteration in instrumental configuration save for the apparatus necessary for temperature control. Good significance can therefore be attached to these values (the consistency is exemplified by the zero-point errors which are constant to within 0.025° (Table I)). The variations in the lattice constants as a function of temperature are displayed in Fig. 6. The form of these plots, with small expansivity at low temperature followed by an increase above ~270 K, is typical of relatively refractory materials. From the regions above 300 K, the thermal expansion coefficients, α, may be estimated. The derived values of $\alpha_a = 5.9 \times 10^{-6}\ K^{-1}$ and $\alpha_c = 3.5 \times 10^{-6}\ K^{-1}$ are lower than those for sodium β-alumina ($\alpha_a = 8.0 \times 10^{-6}\ K^{-1}$, $\alpha_c = 8.1 \times 10^{-6}\ K^{-1}$ (*34*)) which probably reflects the differing atomic arrangements within the mirror planes.

Second, in addition to those reflections resulting from silver metal and the furnace, further peaks were apparent in the $(I_{obs} - I_{calc})$ difference profiles at both 573 and 720 K. These additional peaks could be satisfactorily indexed on the unit cell of corundum, α-Al_2O_3 (Fig. 7). This assignment was confirmed by an intensity fit to these peaks. When the structure of $DAl_{11}O_{17}$ at 573 K had been completely refined (with exclusion of the 3.8° to which α-Al_2O_3 reflections contributed significant intensity), the entire profile was recalculated. From the resulting values of $(I_{obs} - I_{calc})$ at each point, a partial observed profile for α-Al_2O_3 could be determined and analysed by profile refinement. Atomic parameters were taken from Newnham and De Haan (*35*) and only the unit cell constants were refined because of the limitations of the data

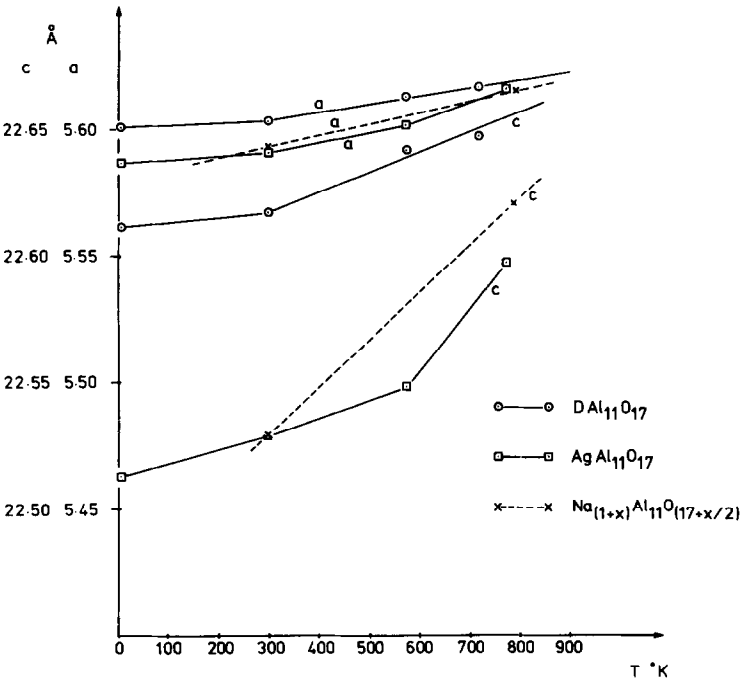

FIG. 6. The lattice constants of $DAl_{11}O_{17}$ and $AgAl_{11}O_{17}$ (Refs. (*8, 22, 33*)) plotted as a function of temperature. The dashed lines indicate the behavior of the nonstoichiometric sodium compound as calculated using the data of Peters *et al.* (*2*) and May and Henderson (*34*).

set. Values of $a = 4.765(2)$ Å and $c = 13.015(4)$ Å were obtained

This result exemplifies two of the advantages of the profile refinement technique. First, impurity phases can be well-characterized *in situ*. Indeed they may even be employed as an internal wavelength calibrant (*8*). Second, although in the case

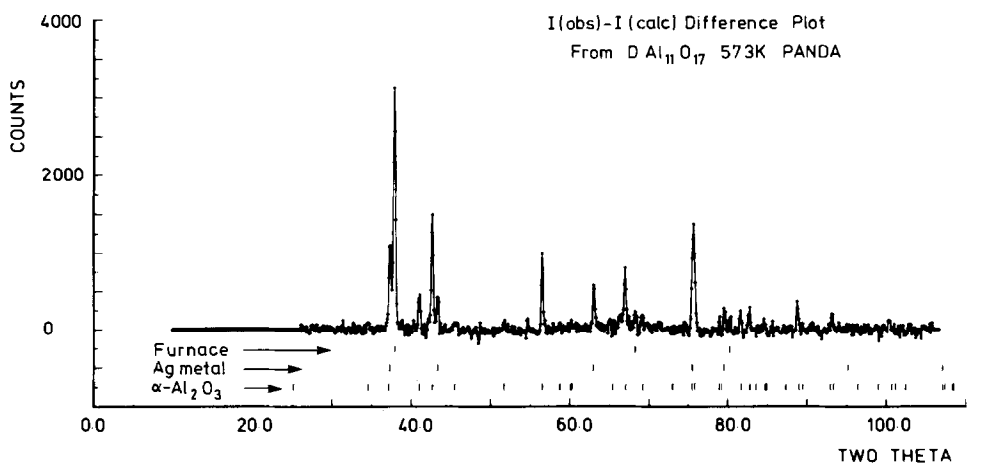

FIG. 7. A plot of the difference between the observed and calculated profiles for $DAl_{11}O_{17}$ at 573 K. The positions and assignments of the additional reflections are marked.

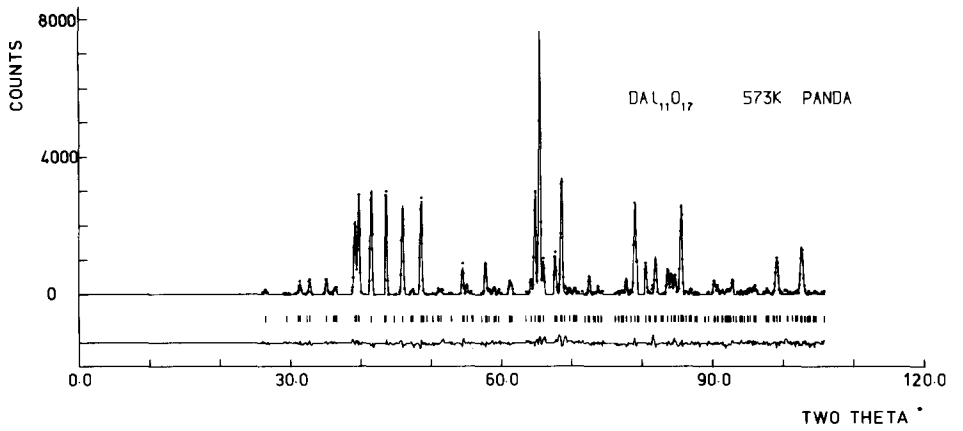

FIG. 8. Final observed, calculated, and difference diffraction profiles for $DAl_{11}O_{17}$ at 573 K (legend as for Fig. 3).

described here Bragg reflections from three different impurities are superimposed on the principal pattern, the structure of the predominant phase can still be well determined. Because the peak shapes are well described, it is not necessary that the entire Bragg peak be resolved. Peaks from α-Al_2O_3 were not observed in either of the lower temperature scans (Figs. 3 and 4).

The deuterium location and iterative structure refinement were achieved in the manner outlined above. After a satisfactory convergence had been obtained with isotropic temperature factors, anisotropic components were introduced for O(5) and D. Fully anisotropic refinement was also possible (*33*) although with little improvement in the residuals.

The D and O(5) positions were again probed in detail by repeating refinements for combinations of D at $x\ \bar{x}\ \frac{1}{4}$ (6*h*) or $x\ y\ \frac{1}{4}$ (12*j*) and O(5) at $x\ \bar{x}\ \frac{1}{4}$ (6*h*) (with $x < \frac{1}{3}$ and $x > \frac{1}{3}$) or $x\ y\ \frac{1}{4}$ (12*j*). The merits of the different models were compared by reference to the profile residuals, bond lengths, number of variables and consistency with the other data sets. The results of several of the refinements were quite similar, but the model

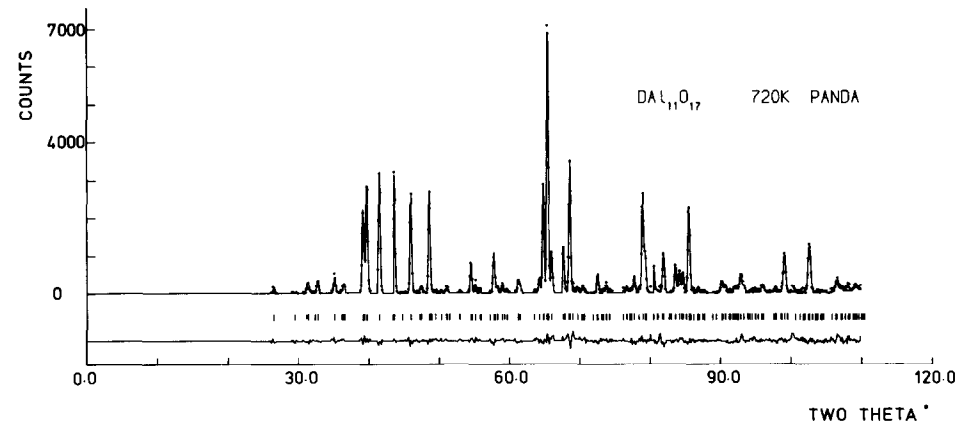

FIG. 9. The final observed, calculated, and difference diffraction profiles for $DAl_{11}O_{17}$ at 720 K (legend as for Fig. 3).

with both D and O(5) on 6*h* sites, with $x_O < \frac{1}{3}$, was selected on the basis of these criteria (Tables II–IV, Figs. 8, 9).

In the earlier stages, the possibilities both of occupation by D of sites other than close to $x\ \bar{x}\ \frac{1}{4}$ (6*h*) with $x \simeq 0.5$, and of partial reverse exchange to $(Ag/D)Al_{11}O_{17}$ were explored. There was no evidence for the former, but occupation numbers greater than zero could be obtained for silver entered at the stoichiometric position $x\ \bar{x}\ \frac{1}{4}$ (6*h*) with $x = -0.236$ (*8, 22*). The maximum values realized were 0.24(9) at 573 K and 0.15(8) at 720 K. These values border on significance, but while some reverse exchange will undoubtedly occur, with the liberation of D_2, the reaction will be limitied by the pressure of this D_2 gas which is contained by the sample can. The low occupation numbers for Ag (scattering length b = 0.60×10^{-14} m), the values obtained for the deuterium occupancy ($b = 0.667 \times 10^{-14}$ m), and the intensity of the Ag_m reflections in the observed diffraction profile show that the extent of this process must be slight. The silver site was therefore not included in the later stages of refinement. Population of another site ($x\ \bar{x}\ \frac{1}{4}$ (6*h*) with $x = 0.91$) close to the mid-oxygen position was also considered. Some Fourier syntheses (Fig. 10) did appear to indicate possible occupation of this site, but the refined occupancies of 0.03(5) (298 K), 0.30(8) (573 K), and 0.02(5) (720 K) could again not overall be regarded as significant.

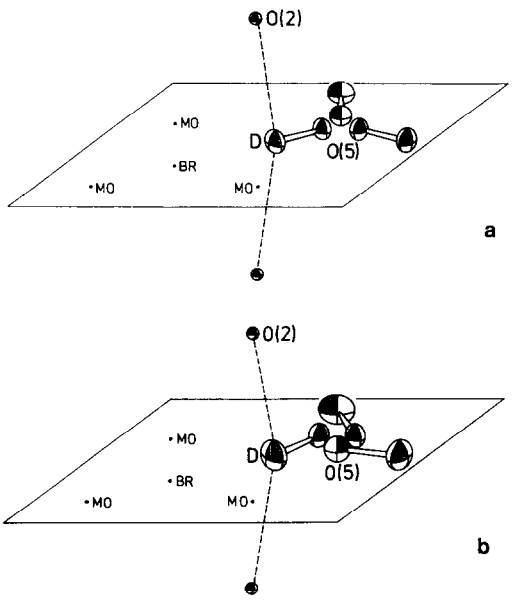

FIG. 11. The distributions of atomic density about the $z = \frac{1}{4}$ plane of $DAl_{11}O_{17}$ at 298 K (upper) and 573 K (lower) drawn with the assistance of the ORTEP program (compare Fig. 1 and see Table II footnote (*e*)). Only one of the three crystallographically equivalent pairs of D and O(5) sites will be occupied in any given mirror plane.

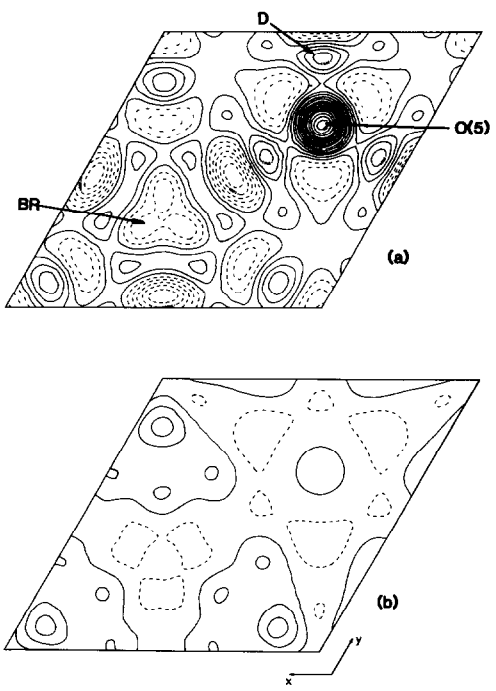

FIG. 10. The $z = \frac{1}{4}$ sections of $|F_{obs}|$ ((a) upper) and $|F_{obs} - F_{calc}|$ ((b) lower) Fourier syntheses using structure factors derived from the final profile refinements of $DAl_{11}O_{17}$ at 720 K (details as for Fig. 2).

The final observed Fourier section for the 720 K data, shown in Fig. 10, is somewhat ill-defined. This derives both from the factors discussed above and from inaccuracies in some of the "observed" structure fac-

tors which result from overlap with regions which were excluded because of the impurities. Even at the end of the analysis, the $/F_{obs}/$ synthesis thus does not accurately depict the structural model which the data provides (Fig. 11). All Fourier calculations based on powder data are subject to these types of uncertainties. In using profile analysis, therefore, it is generally advisable to explore all structural possibilities in iterative least-squares refinements, as outlined above for the present system.

4. Conclusion

As with the previous study of $DAl_{11}O_{17}$ (*20*), the present structural analysis does not indicate the stoichiometry of deuterium β-alumina with high precision. However, taken overall, the earlier work, our accurate analysis of $AgAl_{11}O_{17}$ (*8*), and the consistency of the present results indicate that the product of the reduction of polycrystalline silver β-alumina by D_2 at 450° has the stoichiometric composition, $DAl_{11}O_{17}$. At each of the temperatures studied, all the sites normally occupied by cations in metal β-aluminas are vacant and there are no mirror-plane species other than the spacer oxygen, O(5), and the deuterium. The material is anhydrous.

It has been difficult to establish whether such apparently crystallographically perfect anhydrous hydrogen β-alumina may be prepared by the thermal decomposition of ammonium β-alumina (*10, 36–38*). In the present preparation we have demonstrated that interstitial O_i species are lost as water at 450°C. In hydrogen-containing β-alumina prepared by the action of sulfuric acid on sodium β-alumina, final water loss to, apparently, $HAl_{11}O_{17}$ does not occur until ca. 700°C (*39*).

For $DAl_{11}O_{17}$ at 4.2 K our analysis broadly confirms the earlier work (*20*). The deuterium is closely bonded to the spacer oxygen in a hydroxyl linkage, both atoms being well localized in threefold 6*h* sites about the 2*c* position. This arrangement is presumably favored by weak electrostatic interactions between the deuterium and the two neighboring O(2) ions at a distance of 2.4 Å. At 298 K, the atomic distribution is essentially unchanged. At temperatures above ambient, 573 and 720 K, there is marginal evidence for slight delocalization of deuterium away from the 6*h* sites, but the strong hydroxyl linkage to O(5) is maintained. It therefore seems unlikely that this material will support appreciable protonic conductivity. The similarity of the structure at the four temperatures studied is in marked contrast to the behavior of both stoichiometric (*8, 22, 40*) and nonstoichiometric (*41*) metal β-aluminas. There are, however, some minor variations. For the 6*h* deuterium site, $x\ \bar{x}\ \frac{1}{4}$, the value of x decreases in a continuous fashion (Table II). The variation is such that in the interpretation of the diffraction data, we were obliged to consider the O(5) displacements at 573 and 720 K in an opposite sense to those at 4.2 and 298 K in order to maintain a D–O separation of ca. 1 Å. The diffraction data do not allow a distinction between this possibility and that of a continuous change in D–O bond length with temperature, although the latter would appear unlikely.

In keeping with the previous observations (*20*), we find that the Al(3)–O(5) distance is increased, and the Al(3)–O(2) distance decreased relative to normal metal β-aluminas. The decrease in Al(3)–O(2) is particularly pronounced. These changes reflect the absence of cation density around the *BR* site, the effect of the O(5)–D linkage and, to a lesser extent, the apparent absence of interstitial aluminiums. The coordination of Al(1) is unremarkable. The Al(1)–O(2) distance differs little from that in other β-aluminas. The Al(1)–O(4) separation is marginally reduced, but the magnitude of the variation is probably insignificant.

The alumina observed at 573 and 720 K is presumably formed by the reaction

$$2DAl_{11}O_{17} \rightarrow D_2O + 11Al_2O_3.$$

This decomposition apparently occurred at 573 K, although the intensity of α-Al_2O_3 reflections did not change significantly as the sample was maintained at 573 K, and then 720 K, for several days. The extent of the reaction will be limited by the pressure of D_2O gas within the sample can, and the effectiveness of the sealing system was evidenced by the negligible extent of back-exchange to $AgAl_{11}O_{17}$. This is a relatively low temperature for the formation of α-Al_2O_3. Diaspore, for example, decomposes to α-Al_2O_3 only above ca. 673 K (*42*). The specialized conditions of the present experiment do not allow a direct comparison with other hydrogen-containing β-aluminas, although it is clearly possible that the production of "$HAl_{11}O_{17}$" by high temperature routes, such as the decomposition of the ammonium compound, may be accompanied by a similar degradation. A reduction in the crystal perfection of such material is evidenced in both neutron diffraction studies (*37*) and electron lattice imaging (*43*). No significant presence of α-Al_2O_3 is observed, however, in studies up to 900°C of the thermal decomposition of ammonium β-alumina in which irreversible decomposition only beings to occur near 700°C.

Acknowledgments

We are indebted to C. F. Sampson for assistance in sample preparation, to W. Futcher for help with the neutron diffraction experiments, to W. A. England for access to the original data set, and to the Science Research Council for the provision of neutron scattering facilities. JMN acknowledges financial support by AERE Harwell under the terms of Research Contract H4B 2952 EMR.

References

1. Y. F. Yao and J. T. Kummer, *J. Inorg. Nucl. Chem.* **29,** 2453 (1967).
2. C. R. Peters, M. Bettman, J. W. Moore, and M. D. Glick, *Acta Crystallogr. B* **27,** 1826 (1971).
3. B. C. Tofield, *in* "Intercalation Chemistry" (M. Whittingham and A. J. Jacobson, Eds.), pp. 181–227, Academic Press, New York (1982).
4. J. M. Newsam and B. C. Tofield, *in* "Fast Ionic Transport in Solids" (J. B. Bates and G. C. Farrington, Eds.), North–Holland, Amsterdam (1981); *Solid State Ionics* **5,** 59 (1981).
5. M. A. M. Bourke, A. Hooper, P. T. Moseley, and R. G. Taylor, *Solid State Ionics* **1,** 367 (1980).
6. W. L. Roth, *J. Solid State Chem.* **4,** 60 (1972).
7. J. P. Boilot, Ph. Colomban, G. Collin, and R. Comes, *J. Phys. Chem. Solids* **41,** 47 (1980).
8. J. M. Newsam and B. C. Tofield, *J. Phys. C* **14,** 1545 (1981).
9. J. T. Kummer, *Prog. Solid State Chem.* **7,** 141 (1972).
10. B. A. Bellamy, A. Hooper, A. E. Hughes, J. M. Newsam, C. F. Sampson, and B. C. Tofield, *in* "Energy and Ceramics" (P. Vincenzini, Ed.), pp. 950–963, Elsevier, Amsterdam (1980).
11. Ph. Colomban and A. Novak, *in* "Solid State Protonic Conductors" (J. Jensen and M. Kleitz, Eds.), pp. 183–201, Odense Univ. Press, Odense (1982).
12. K. G. Frase, G. C. Farrington, and J. O. Thomas, *Ann. Rev. Mater. Sci.* **14,** 279 (1984).
13. J. P. Boilot, Ph. Colomban, G. Collin, and R. Comes, *in* "Fast Ion Transport in Solids" (P. Vashishta, J. N. Mundy, and G. K. Shenoy, Eds.), p. 243, Elsevier/North–Holland, New York (1979).
14. W. A. England, B. C. Tofield, and A. J. Jacobson, *J. Chem. Soc. Chem. Commun.*, 895 (1976).
15. G. C. Farrington and J. L. Briant, *Mater. Res. Bull.* **13,** 763 (1978).
16. L. Glasser, *Chem. Rev.* **75,** 21 (1975).
17. A. Potier and D. Rousselet, *J. Chim. Phys.* **70,** 873 (1973).
18. M. G. Shilton and A. T. Howe, *Mater. Res. Bull.* **12,** 701 (1977).
19. W. Hayes, L. Holden, and B. C. Tofield, *J. Phys. C* **13,** 4217 (1981).
20. B. C. Tofield, A. J. Jacobson, W. A. England, P. J. Clarke, and M. W. Thomas, *J. Solid State Chem.* **30,** 1 (1979).
21. J. M. Newsam, B. C. Tofield, W. A. England, and A. J. Jacobson, *in* "Fast Ion Transport in Solids" (P. Vashishta, J. N. Mundy, and G. K. Shenoy, Eds.), p. 405, Elsevier/North–Holland, New York (1979).
22. J. M. Newsam, B. C. Tofield, A. K. Cheetham, and A. W. Hewat, in preparation.

23. W. HAYES, L. HOLDEN, AND B. C. TOFIELD, *Solid State Ionics* **1,** 373 (1980).
24. H. M. RIETVELD, *J. Appl. Crystallogr.* **2,** 65 (1969).
25. T. M. SABINE AND P. J. CLARKE, *J. Appl. Crystallogr.* **10,** 277 (1977).
26. P. J. CLARKE, "Oxford Rietveld Refinements User Manual," unpublished (1976).
27. L. KOESTER, *in* "Neutron Physics," Springer Tracts in Modern Physics, Vol. 80 (O. Hohler, Ed.), p. 1–55, Springer-Verlag, Berlin (1977).
28. G. E. BACON, *Acta Crystallogr. A* **28,** 357 (1972); *ibid.* **30,** 847 (1974).
29. J. M. ADAMS, R. G. PRITCHARD, AND A. W. HEWAT, *Acta Crystallogr. B* **35,** 1759 (1979).
30. A. NOVAK, *Stucture and Bonding* **18,** 177 (1974).
31. K. KATO AND H. SAALFELD, *Acta Crystallogr. B* **33,** 1596 (1977).
32. The data of Ref. (*30*) were re-refined by F. REIDINGER, Ph.D. thesis, SUNY, Albany (1979).
33. J. M. NEWSAM, D. Phil. thesis, Oxford (1980).
34. G. J. MAY AND C. M. B. HENDERSON, *J. Mater. Sci.* **14,** 1229 (1979).
35. R. E. NEWNHAM AND Y. M. DE HAAN, *Z. Krist.* **117,** 235 (1962).
36. B. C. TOFIELD, J. M. NEWSAM, AND A. HOOPER, *in* "Fast Ionic Transport in Solids" (J. B. Bates and G. C. Farrington, Eds.), North–Holland, Amsterdam (1981); *Solid State Ionics* **5,** 249 (1981).
37. J. M. NEWSAM, A. K. CHEETHAM, AND B. C. TOFIELD, *Solid State Ionics* **8,** 133 (1983).
38. PH. COLOMBAN, J. P. BOILOT, A. KAHN, AND G. LUCAZEAU, *Nouv. J. Chim.* **2,** 21 (1978).
39. W. L. ROTH, M. W. BREITER, AND G. C. FARRINGTON, *J. Solid State Chem.* **24,** 321 (1978).
40. J. P. BOILOT, PH. COLOMBAN, R. COLLONGUES, G. COLLIN, AND R. COMES, *J. Phys. Chem. Solids* **41,** 253 (1980).
41. J. P. BOILOT, J. THERY, R. COLLONGUES, R. COMES, AND A. GUINIER, *Acta Crystallogr. A* **32,** 250 (1976).
42. For a review see C. N. SATTERFIELD, *in* "Heterogeneous Catalysis in Practice," pp. 88ff., McGraw–Hill, New York (1980).
43. Such an image collected by P. T. MOSELEY is shown in Ref. (*3*).